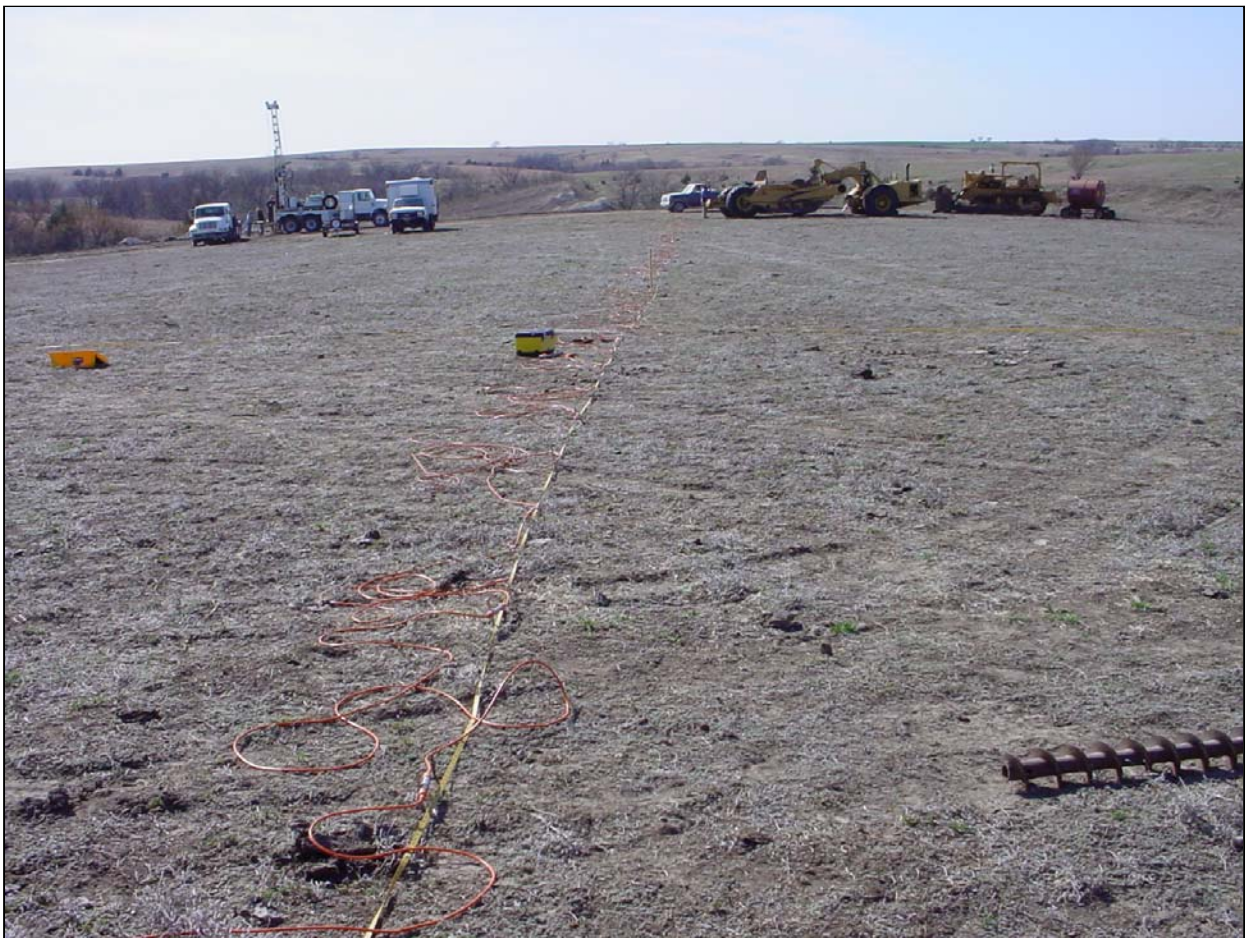# Feasibility of Delineating a Volcanic Ash Body Using Electrical Resistivity Profiling

Jianghai Xia
Greg Ludvigson
Richard D. Miller
Lindsay Mayer
Adel Haj

Kansas Geological Survey
1930 Constant Avenue
Lawrence, KS 66047

Report to
John M. Boley, Kansas Minerals Inc., 1886 Q Road, Mankato, KS 66956

Feasibility of Delineating a Volcanic Ash Body Using Electrical Resistivity Profiling

by

Jianghai Xia
Greg Ludvigson
Richard D. Miller
Lindsay Mayer
and
Adel Haj

Kansas Geological Survey
The University of Kansas
1930 Constant Ave.
Lawrence, KS 66046

Report to

John M. Boley
Kansas Minerals Inc.
1886 Q Road
Mankato, Kansas 66956

October 2010

KGS Open-file Report No. 2010-14

Feasibility of Delineating a Volcanic Ash Body Using Electrical Resistivity Profiling

Jianghai Xia, Greg Ludvigson, Richard D. Miller, Lindsay Mayer, and Adel Haj

Volcanic ash production in Kansas has not lived up to its potential since limited production began in the early 1900s (Hardy et al., 1965). Between 1920 and 1940 Kansas was the largest producer of volcanic ash products in the US. Since 1945, commercial production has steadily declined and in 1960 only two producers operated in Kansas. Applications and therefore markets exist for both raw and popped or bloated ash products. Uses for refined ash include filtrate media, plaster wallboard, thermal (low-temperature) insulation, and lightweight fireproof acoustic tile. Markets for raw ash include: ceramic components, glass products, mild abrasives, road construction, concrete aggregate, and as a component of granular fertilizer. Both bloated and raw ash have been used as oil and grease absorbents and inert filters.

Key to exploiting this resource is identification of viable products and associated markets for the raw and processed material. However, before this near-surface product can be marketed, viable means must be developed for estimated volumes, geometries, and characteristics of the ash deposits. Most important is the development of cost-effective techniques for locating, sampling (for assay), and delineating volcanic ash deposits with great enough certainty to allow the accurate resource projections necessary for securing long-term contracts based on known reserves and thereby deliverable product.

Exploitation of volcanic ash deposits currently mined in northern Kansas has been limited to sparse subsurface data from drill cuttings and exposures in shallow pit walls. Continued extraction of ore from operating mines has been guided by operator observations of successive fresh exposures that appear during the mining process, interpolated to the nearest drill hole with cuttings. To estimate mineable tonnage and characteristics of ore, the geometry of the ore body(ies) must be delineated and representative, and intact samples extracted for assay. To ensure the highest accuracy and reliability of these estimations, drill holes need to be optimally placed to allow reliable extrapolations from these borings within a threshold percentage.

With so little known about the site-specific geology and the characteristics of the ash as well as the overburden and basal contact, an integrated geophysical (electrical resistivity, magnetic, and ground penetration radar) survey was conducted with borehole verifications in search of these ore bodies. Both geophysical test data and borehole samples were acquired at sites in close proximity to an existing mine face. Electrical resistivity profiling provides most encouraging results in delineating volcanic ash bodies and addressing the following questions.

Site Geology

Drillcore 1 (B1) near the western end of the studied area was drilled several meters back from the position of the mine high wall. This drillcore penetrated 15 ft of volcanic ash—the ore body being mined at the site (Figure 1). Field studies were carried out along the high wall. This field sampling also produced high quality samples of the ash bed sedimentology through the quarrying of sediment sample monoliths that will be the subjects of subsequent laboratory studies.

Drillcore 2 (B2) near the eastern end of the studied area was drilled several meters from a fence line that delimits the leased property for mining activity. This drillcore penetrated less than 1 meter of impure volcanic ash, clearly showing that mineable ash bed resources do not extend throughout the whole extent of the leased property (Figure 1).

Figure 1 also shows interpretations of the sedimentologic and stratigraphic relationships between the three observation points at the mine site discussed above, also integrated with results from later drilling and electric resistivity profiling. The mined ash bed is interpreted to be a valley-filling deposit of stream and ponded volcanic ash sediments that were eroded from the primary direct air-fall volcanic ash sediments that were originally deposited in upland positions on the landscape. These later stream-related processes led to a thickening of volcanic ash sediments at their sites of secondary deposition. The succession of alluvial (stream-laid) sediments accumulated on a valley floor that was inset (cut by stream incision) from the upland stratigraphy shown by B2 (Figure 1).

The boundaries of the mineable ash bed resources are limited by the positions of buried *cutbank scarps* (Figure 1), steeply inclined former stream banks that were cut downward into the upland stratigraphy and cut even further downward into the chalks of the Niobrara formation, the local Cretaceous bedrock. These cutbank scarps bound the thick ash deposit currently being mined and a thinner ash deposit that rests on a higher buried stream terrace level to the east of the mine. The electric resistivity profiling proved to be very successful in imaging the location of the buried cutbank scarps.

One local complication in the site geology relates to the distribution of colluvial deposits that are exposed above the ash deposit at the northern end of the mine high wall. This colluvium consists of fragments of weathered Cretaceous chalk and Cretaceous marine mollusk fossils all within a sandy matrix. These deposits were weathered and transported from the local Cretaceous bedrock in higher landscape positions above the mine site. They were also encountered in drill-core B1 and borehole H4, where they apparently truncated the thin ash deposits on the buried terrace level (Figure 1) in a small-buried gully that cut through and locally removed the ash deposits.

Background of electrical resistivity profiling

Two-dimensional (2D) electrical resistivity profiling (ERP) at the surface is normally used to estimate the subsurface electric resistivity distribution by taking measurements along a survey line. Each measurement generally requires electrical current to be injected into the ground through two current-carrying electrodes with voltage measurements taken at two potential electrodes some specific distance away. An apparent resistivity is calculated using the injected current, the measured voltage, and a geometric factor related to the arrangement of the four electrodes (Zohdy et al., 1974; Reynolds, 1997). The maximum investigation depth of electrical resistivity depends generally on the spacing of the current injecting electrodes. Therefore, sampling different depths is accomplished by changing the electrode spacing. Individual measurements are taken along a survey line using various combinations of electrodes and spacings to produce an apparent resistivity cross section. Apparent resistivity is an averaged value with contribution from both horizontal and vertical directions effectively reducing resolution of ERP results with increasing investigation depths.
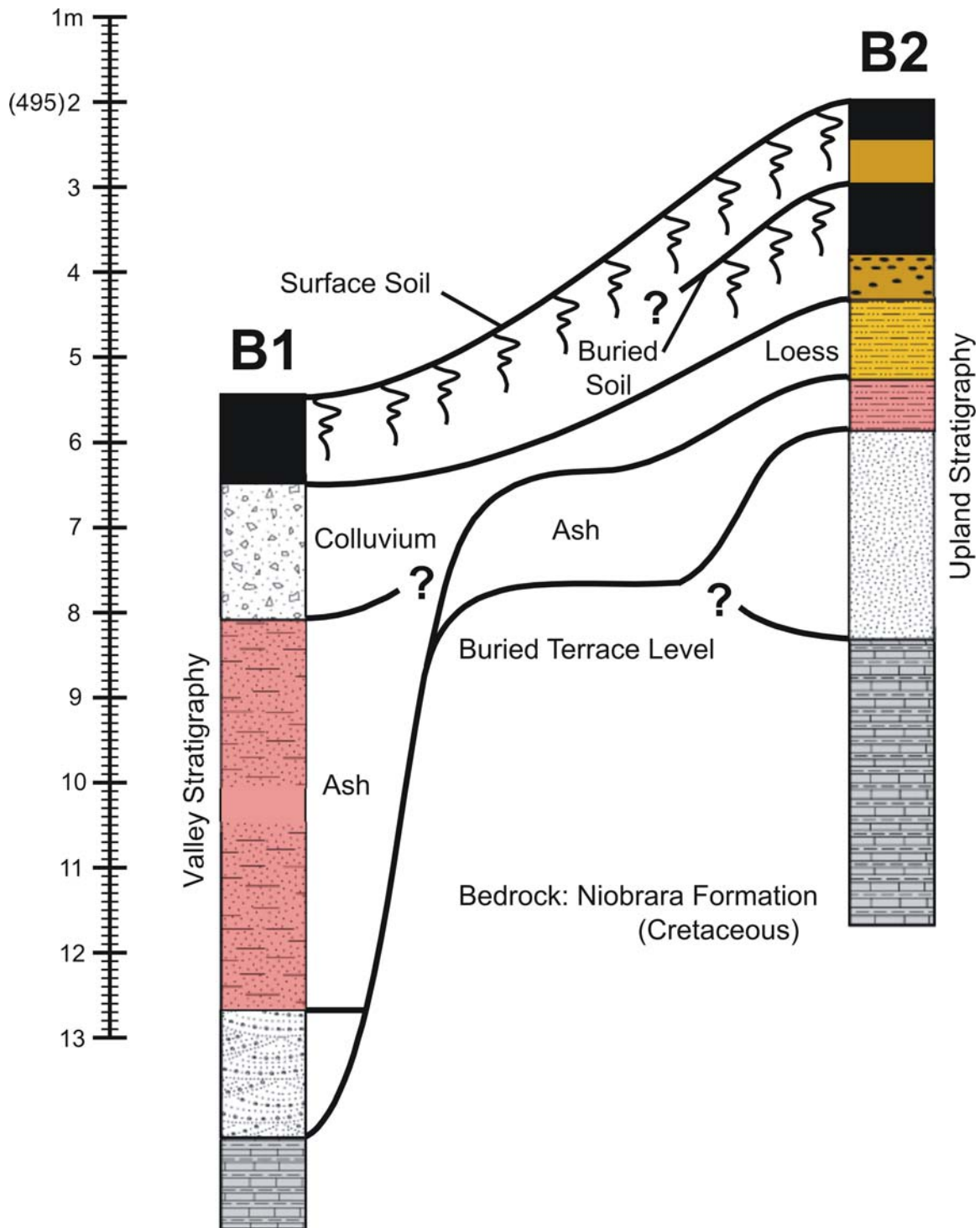
Figure 1. Borehole logs at the mine site, with interpretations of sedimentologic and stratigraphic relationships between the deposits. Steep boundaries limiting the extent of the ash deposits are buried cutbank scarps.

Apparent resistivity data are then inverted into an electric resistivity model that practically increases the resolution of the resistivity model and allows interpretation of the subsurface structure and stratigraphy (Wolfe et al., 2000; deGroot-Hedlin and Constable, 1990; Oldenburg and Li, 1999; Tsourlos et al., 1999; Loke, 2001). Many geological/environmental and cultural factors affect or control the apparent measured resistivity of the subsurface, some of these factors include the composition of the subsurface materials, the amount of water in the subsurface, and the ionic concentration of the pore fluid. Electrical resistivity models are commonly used to identify, delineate, and map subsurface features such as electrically conductive contamination plumes, bedrock fracture zones, the saltwater/freshwater contact, the vadose zone, electrically conductive lithologic units such as clay, and sediment size distribution (Dawson et al., 2002; Behiry and Hanafy, 2000; Benson et al., 1997; Xia and Miller, in press).

This feasibility study employed the use of ERP to delineate a volcanic ash body in the north-central Kansas primarily focusing on the question of how well the volcanic ash at this site, known to be present from drill and quarry samples, could be delineated beneath several to tens of feet of soil (Figure 2).

Electric property of volcanic ash

Based on chemical analyses of 54 volcanic ash samples from around Kansas, the chemical composition of volcanic ash from the various deposits around Kansas is remarkably uniform. Fresh volcanic ash samples from Kansas commonly contain more than 70 percent silica (SiO_2), approximately 12 percent alumina (Al_2O_3), 2 percent ferric oxide (Fe_2O_3), 7 percent alkalies, and
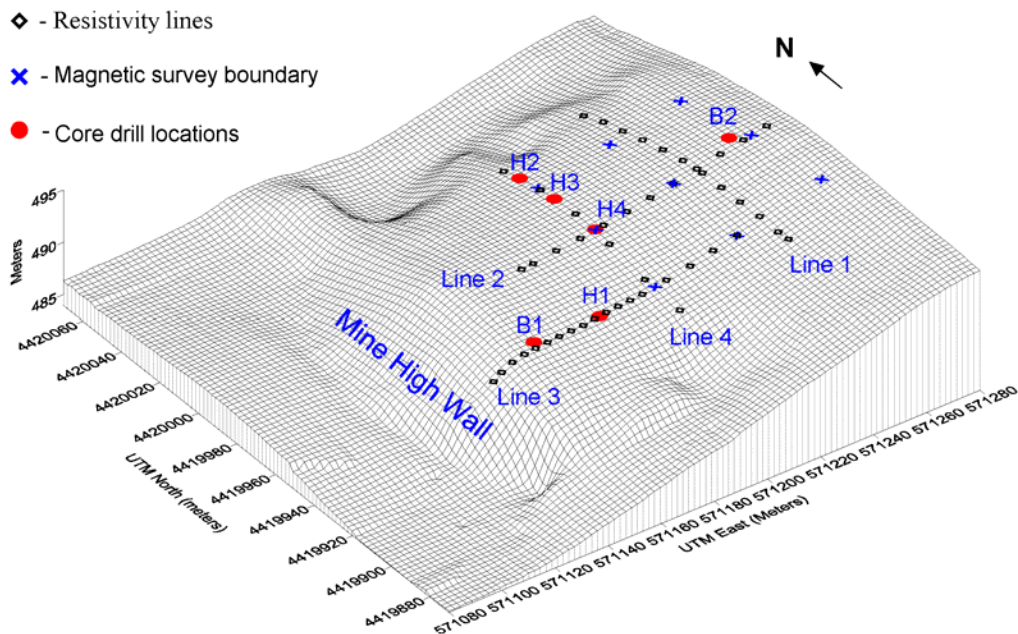

Figure 2. Contour net diagram depicting surface elevation with locations of drill holes and geophysical survey data coordinates.

generally less than 3 percent lime (CaO) and magnesia (MgO) (Carey et al., 1952). Based on these findings, Kansas volcanic ash has a relatively high resistance to the flow of electric current, so a layer of volcanic ash beneath soils should be detectable using ERP surveys. We expect a higher electric resistance for volcanic ash than surrounding materials based on its chemical composition. However, variations in composition due to contaminants such as clay and iron oxide could complicate the volcanic ash's resistivity signature. Borehole information was necessary to calibrate resistivity values associated with volcanic ash and to verify interpretations based on resistivity anomalies.

Electric resistivity surveys and core drilling

ERP surveys were performed along four 315-ft lines (see the cover page) on two different trips to the site using a Jilin University Geopen^{TM} E60C multi-electrode resistivity meter (Figure 3a). Sixty-four electrodes (Figure 3b) on 5-ft intervals were used with a Wenner array acquisition approach (Figure 3c) because a Wenner array possesses a balance among vertical resolution, investigation depth, and acquisition noise (Bernard and Leite, 2004). An electrode is a stainless steel bar 14 in. long and 3/8 in. in diameter (Figure 3b). A 20-layer model with an apparent thickness of 100 ft was selected. During data acquisition of sampling each depth, current electrodes A and B and measurement electrodes M and N are systematically selected by the resistivity meter and moved along a line. Distances AM, MN, and NB of a Wenner array are kept the same when sampling each depth (Figure 3c). Data for lines 1 and 2 were acquired during the first trip to the site with the goal to uniquely measure the electrical signature of volcanic ash. Line 1 is north/south and located at the east end of the survey site with the station at 90 ft intersecting the east/west line 2 at the station at 175 ft. During the data acquisition component of the first trip, two boreholes (B1 and B2) were drilled and sampled (Figure 2).

Stage One

ERP surveys were performed along two 315-ft lines (Lines 1 and 2, Figure 2). The resistivity meter systematically and automatically selects current electrodes and measurement electrodes to sample, based on input survey design and approach. Investigation depths increase with increasing distance between electrodes. The maximum designed investigation depth for this array was around 50 ft to 80 ft (1/6 to 1/4 of the profile length; Edwards, 1977). The surface electric resistivity was relatively uniform and low, making surveys much faster than expected and the data quality high. Measured apparent resistivity data were in a range of 20 to 80 Ohm-m.

Measured apparent resistivity data were inverted using EarthImager^{TM} (AGI, 2005). The ground surface was generally flat with a gentle, uniform slope negating the need for topographic corrections. We selected a smooth model inversion algorithm with the default initial model. Selection of the final inverted models was selected based on the maximum derivative change of the root-mean-square error with respect to the iteration number. Figures 4a and 5a are measured apparent resistivity data used as inputs for the inversion. Figures 4b and 5b are calculated apparent resistivity due to the inverted resistivity models shown in Figures 4c and 5c, respectively. Calculated apparent resistivity data generally fit the measured apparent resistivity data maintaining a relative RMS error between 1.8 and 2.3%.
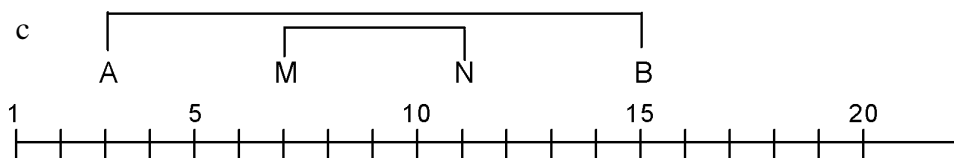
Figure 3. (a) A Geopen[TM] E60C multi-electrode resistivity meter. (b) An electrode, cables and a connector. (c) A Wenner array acquisition approach: Distances AM = MN = NB. Electrodes A and B are current-carrying electrodes with voltage measurements taken at two potential electrodes M and N.
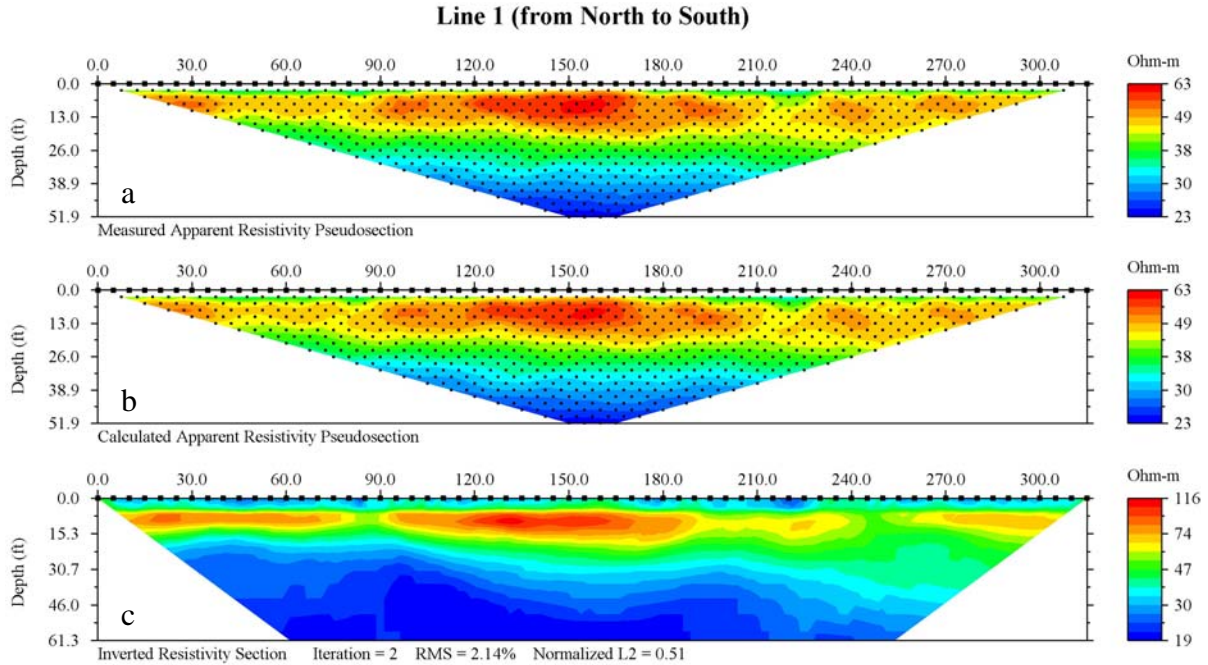
Line 1 (from North to South)

Figure 4. ERP results of line 1. (a) Measured apparent resistivity. Solid squares along the top represent electrodes and dots are data points. (b) Calculated apparent resistivity due to the inverted resistivity models shown in (c). (c) The inverted resistivity model.
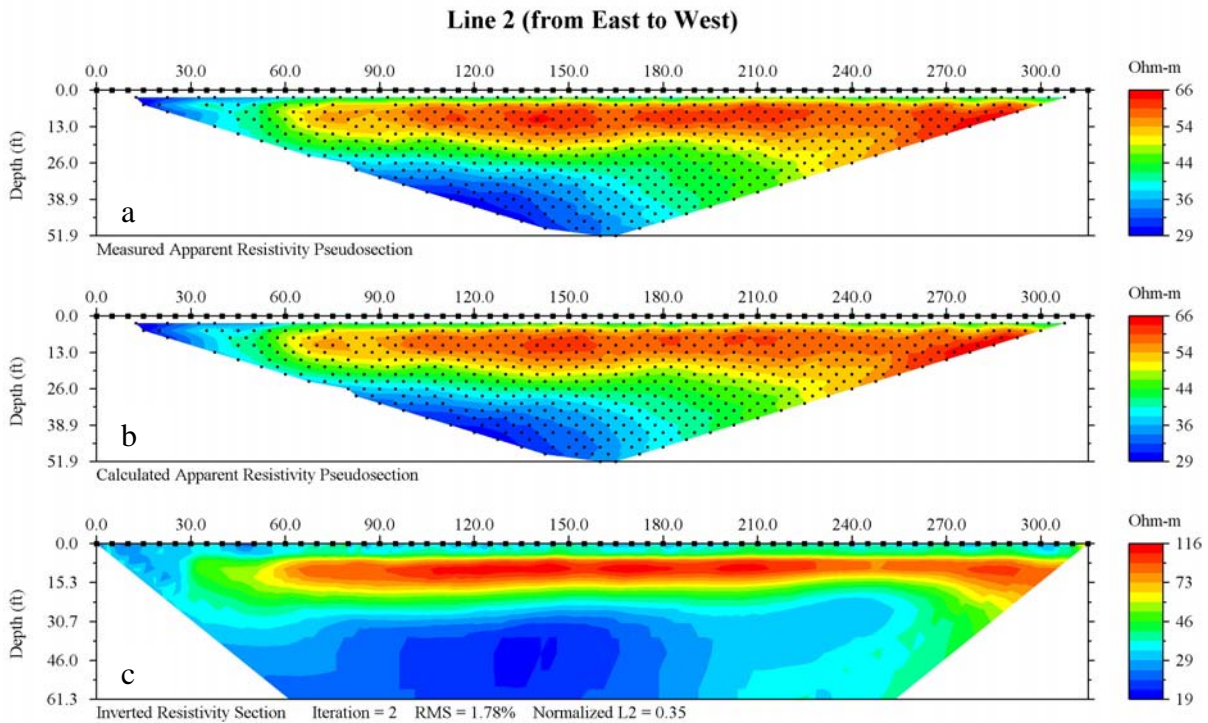

Line 2 (from East to West)

Figure 5. ERP results of line 2. (a) Measured apparent resistivity. Solid squares along the top represent electrodes and dots are data points. (b) Calculated apparent resistivity due to the inverted resistivity models shown in (c). (c) The inverted resistivity model.

Borehole B2 was located 10 ft north of the station at 50 ft on line 2. The borehole geology validated the ERP measurements. A 2.5-ft-thick layer of ash was encountered at a depth of 12 ft, suggesting the high resistivity layer (reddish color on Figures 4c and 5c) could be indicative of volcanic ash at this site. Based on the resistivity data, this layer of volcanic ash appears to thicken to the west (Figure 5c). Using the interpretation of line 2 as a guide, the ERP image along line 1 appears to suggest the volcanic ash layer is discontinuous in the north-south direction (Figure 4c). To confirm these interpretations and tie more ERP images with Borehole B1, two more electric resistivity profiles were acquired during a second stage.

Stage Two

Data along lines 3 and 4 were acquired during stage two of this project to verify consistency and to extend resistivity anomalies interpreted on line 3, and confirmed in Borehole B1 at the station at 250 ft (Figure 2). A 15-ft-thick layer of ash was encountered in Borehole B1 beginning at a depth of 9 ft. Line 3 was an east to west profile with the mine face at the extreme west end of the line, and intersecting line 4 at the station at 100 ft. Line 4 was a north to south profile, perpendicular to line 3, and tied with line 2 at the station at 175 ft and line 3 at the station at 275 ft (Figure 2). The same data acquisition parameters were used to collect these resistivity data as was previously done on lines 1 and 2. The electrical conditions of the ground were generally the same during the acquisition of lines 3 and 4 as when data were collected along lines 1 and 2. Measured apparent resistivity data ranged from 20 to 80 Ohm-m and were consistent with data acquired during stage 1 (Figures 6a and 7a). The same inversion processing approach and initial model was used on line 3 and 4 data as on lines 1 and 2. Figures 6b and 7b display calculated apparent resistivity based on the inverted resistivity models shown in Figures 6c and 7c, respectively.

A higher resistivity layer apparent from station 210 west to the end of line 3 correlates extremely well with mined volcanic ash exposed in the high wall (Figure 6c). Ground truth for line 3 was provided by borehole B1, which was located at the station at 250 ft. One distinguishing feature of this profile (Figure 6c) is the abrupt termination of the higher resistivity layer around the station at 200 ft. This suggests the volcanic ash body as imaged beneath line 3 ends around that station, which is different than what was learned from ERP results of line 2, 100 ft north of line 3. The inverted resistivity model of line 4 (Figure 7c) also suggests this thin layer of volcanic ash terminates to the west around the station at 40 ft.

Inverted resistivity models from the four profiles incorporated with borehole locations (Figure 8) were used to generate the resistivity model fence diagram to provide an image of the volcanic ash layer (Figure 9). Tie points along the profiles correlated extremely well and did not require any depth adjustment to create the inverted resistivity model fence diagram.

Additional borehole verification

To further confirm our interpretation and obtain the ground truth, four additional boreholes were drilled (H1, H2, H3, and H4, Figure 2). Borehole H1 was drilled around the station at 167.5 ft of line 3 and reached total depth (TD) at 25 ft. No ash was found. The relatively low resistivity around the station was due to higher levels of clayey soil. This borehole confirmed that the volcanic ash body terminates around the station at 200 ft on line 3. Borehole H2 was drilled at the station at 30 ft on line 4 and with a TD of 25 ft. About a 1-ft-thick ash layer was
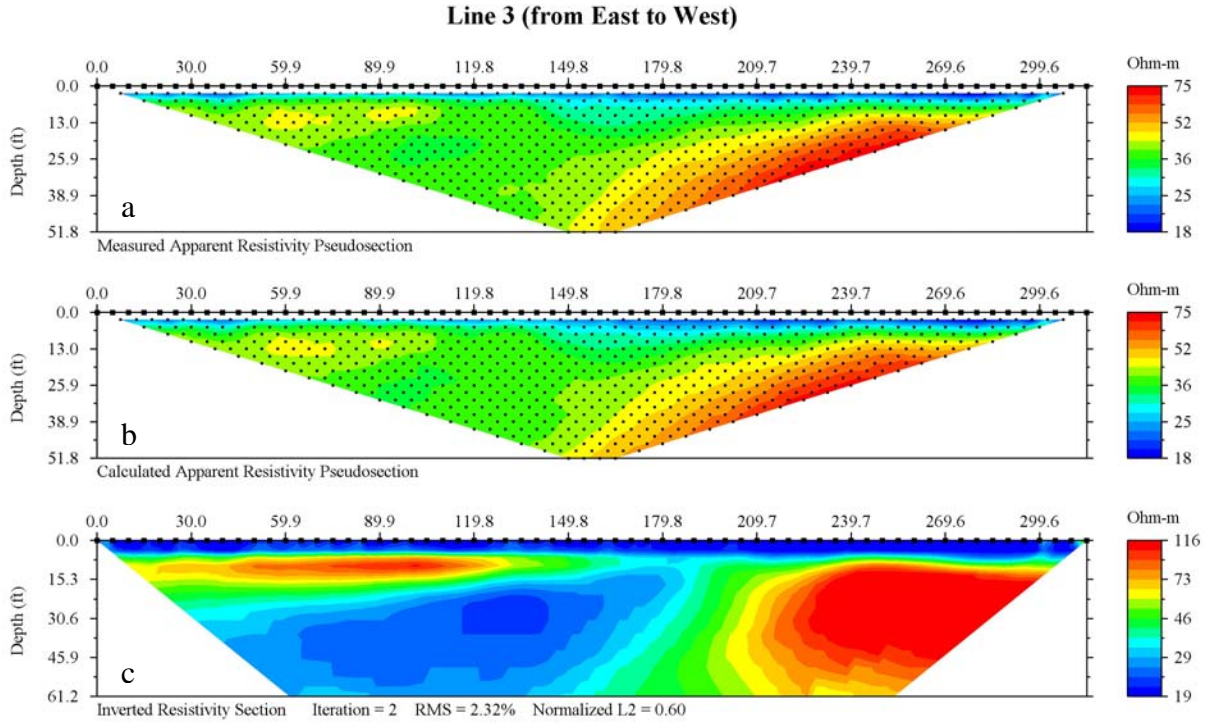
Line 3 (from East to West)

Figure 6. ERP results of line 3. (a) Measured apparent resistivity. Solid squares along the top represent electrodes and dots are data points. (b) Calculated apparent resistivity data due to the inverted resistivity models shown in (c). (c) The inverted resistivity model.
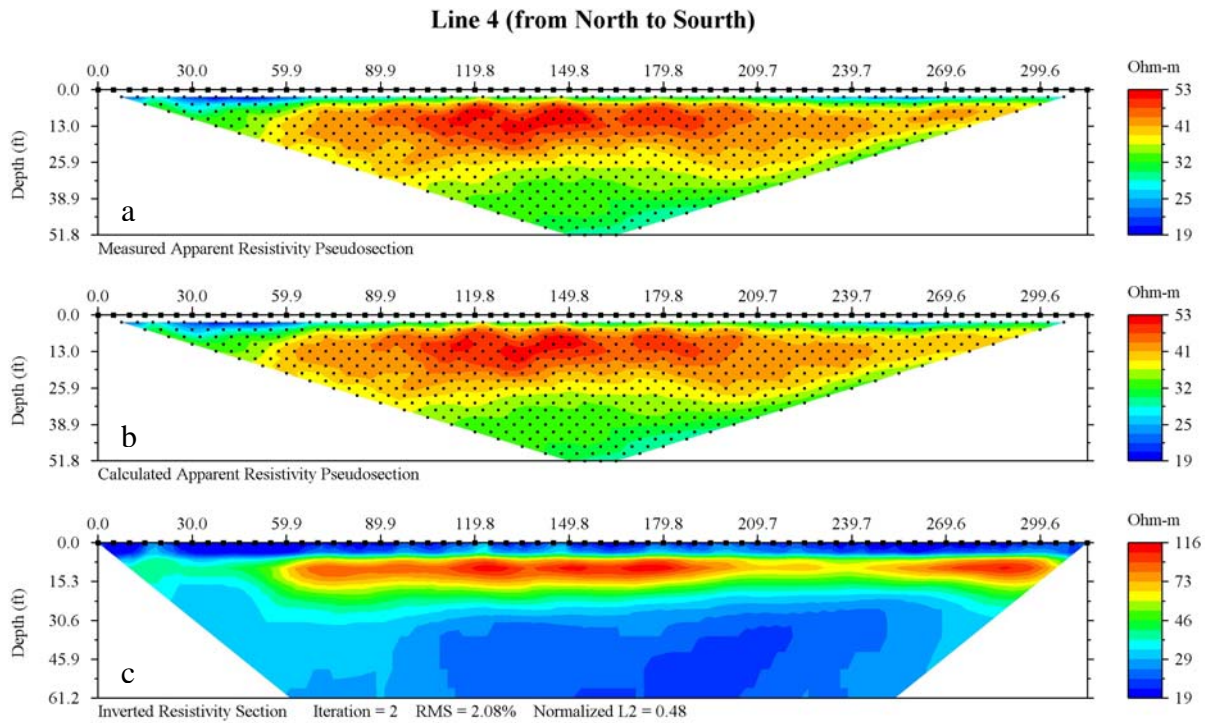
Line 4 (from North to Sourth)

Figure 7. ERP results of line 4. (a) Measured apparent resistivity. Solid squares along the top represent electrodes and dots are data points. (b) Calculated apparent resistivity data due to the inverted resistivity models shown in (c). (c) The inverted resistivity model.
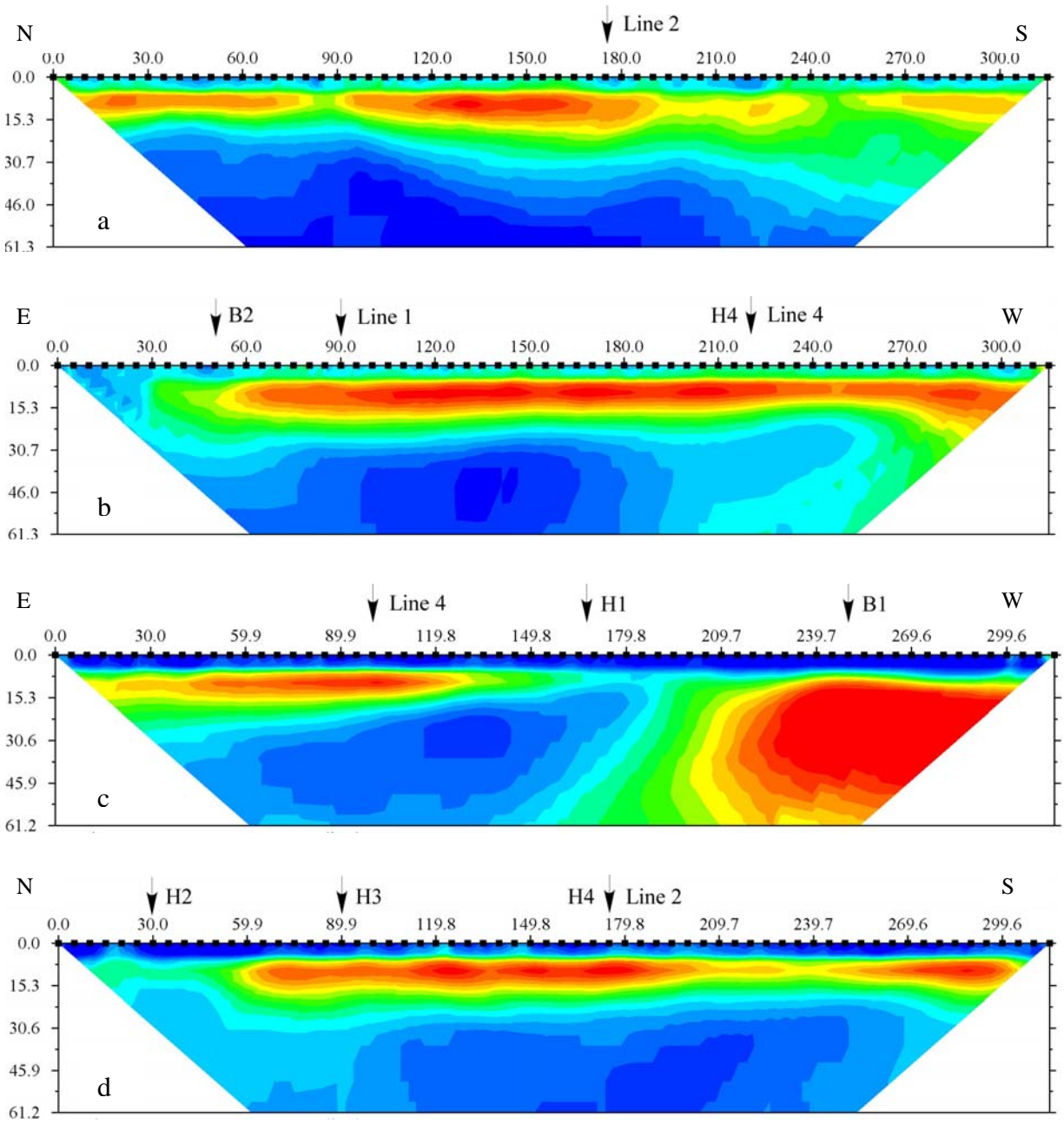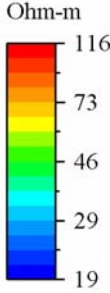
Figure 8. Inverted models with borehole locations and cross-points of tied lines. (a) Inverted resistivity of line 1. (b) Inverted resistivity of line 2. Borehole B2 is located 10 ft north of Line 2. (c) Inverted resistivity of line 3. (d) Inverted resistivity of line 4.
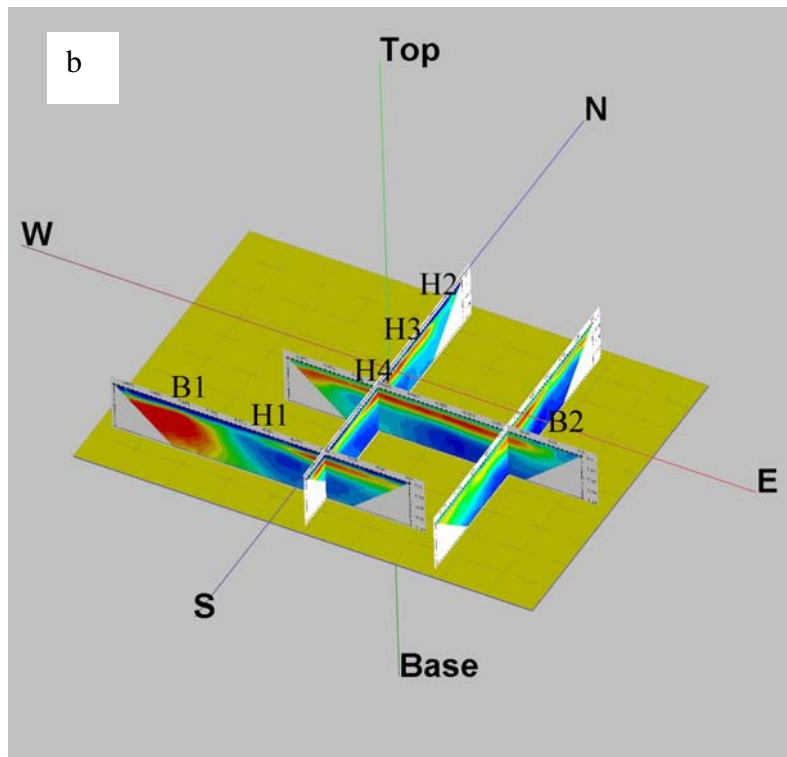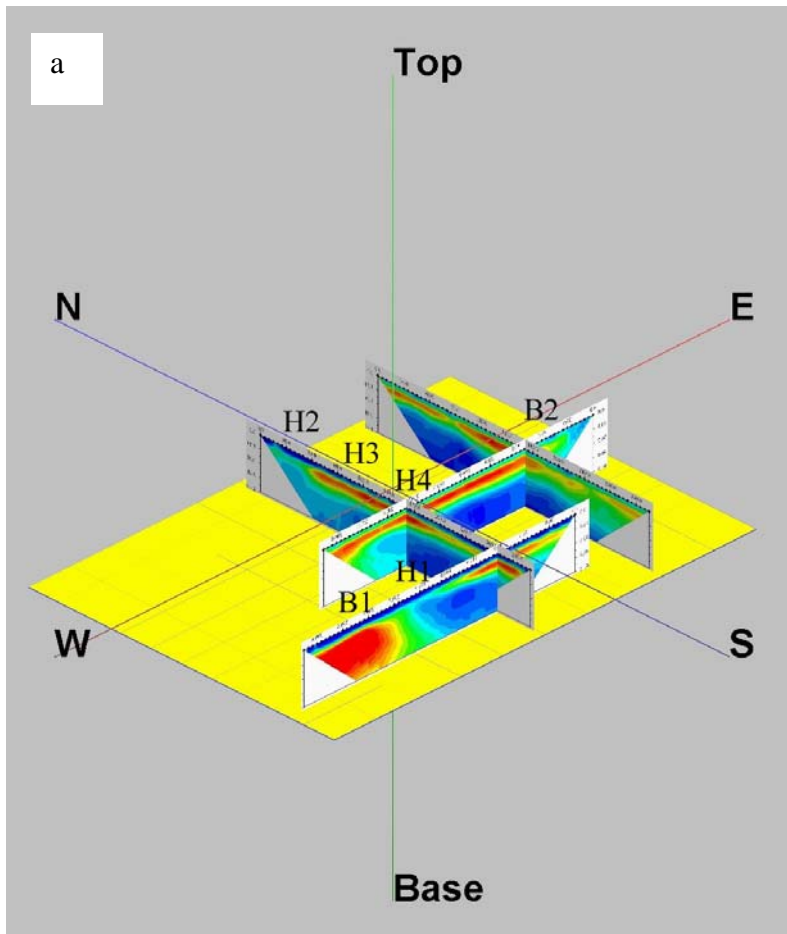
Figure 9. Fence diagrams with borehole locations. (a) A view from the southwest. (b) A view from the southeast.

found at depth between 7-9 ft. Borehole H3 was drilled at the station at 90 ft on line 4 and with a TD of 25 ft. About 5 ft of ash was found at depth between 7 and 13 ft. Borehole results of H2 and H3 confirmed the ERP interpretation that the ash body (a layer in red in Figure 8d) pinches out towards the north along line 4. Borehole H4 was drilled at the station at 175 ft on line 4 with a TD of 25 ft. Borehole samples were recovered from the depth interval between 5 and 11 ft with soil from depth 5 to 7 ft and colluvial deposits from depth 7 to 11 ft. No ash was found in H4 from depth 5 to 11 ft, which is inconsistent with electric resistivity interpretations that suggest volcanic ash should be present at the station at 175 ft on line 4 from depth around 7 to 13 ft as Borehole H3 suggested. A possible reason that the ash is locally missing in H4 is that it was locally cut out by a small gully that was backfilled by the colluvium. This gully might be small enough to have not materially affected the imaging on line 4 due to horizontal smear effects of ERP or volcanic ash could be present at a deeper depth. Drilling results of H2, H3, and H4 indicate a thinner layer (4 to 5 ft) of ash is present between the stations at 80 and 165 ft (Figure 8d).
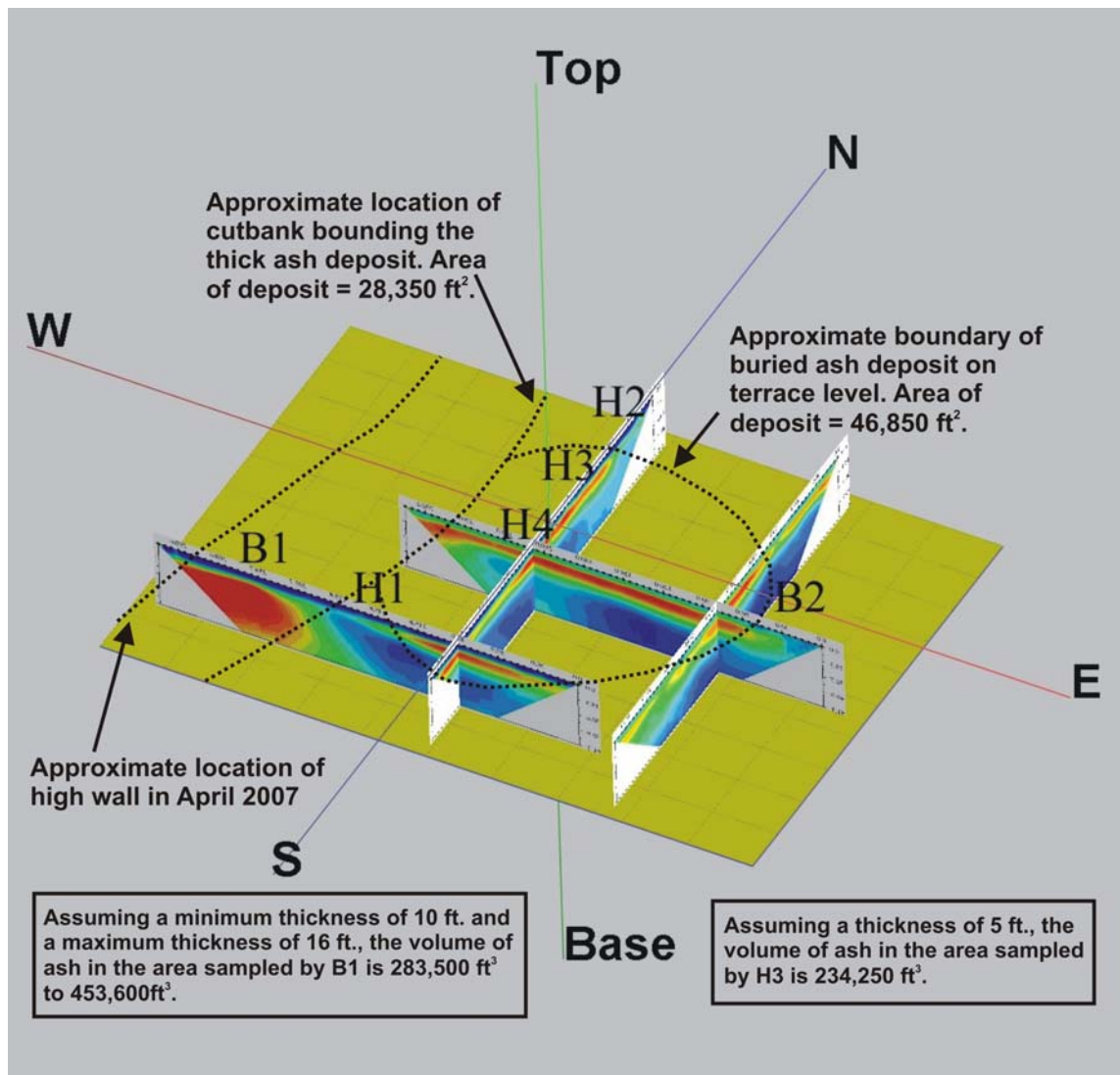

Figure 10. Estimation of the volume of the volcanic ash body based on electric resistivity and borehole results. Dash lines are horizontal boundaries determined by electric resistivity results.

Conclusions

ERP surveys proved to be feasible in defining a drill-confirmed volcanic ash body at this testing site. Due to vertical resolution limits of ERP, the bottom of the ash body is not as clearly defined by inverted resistivity as mine developer would like to see, but the lateral extent and general thickness were clearly determined and confirmed along most lines. With electric resistivity and borehole results, the total volume of ash in the study area would be in the range 518,000 to 688,000 ft^3 assuming the thickness of 10 to 16 ft at Borehole B1 and 5 ft at Borehole H3 (Figure 10).

High-resolution magnetic surveys (Figure 2) and ground-penetration radar (GPR) along lines 1 and 2 were also evaluated at the site. Magnetic anomalies possibly hint at an effective means to delineate the horizontal boundaries of the volcanic ash, but this is yet to be confirmed. The GPR energy penetration was severely limited at this site due to the high conductivity of the surface soil.

Acknowledgments

We thank John Boley of Kansas Minerals Inc. for providing assistance and arrangements for the data acquisition. We also thank Joe Anderson, Brett Wedel, Anthony Wedel, Brett Bennett, Shelby Walters, Joe Kearns, and Justin Schwarzer of the Kansas Geological Survey for acquiring electric resistivity data and GPS data and for performing borehole verifications.

References

AGI, 2005, EarthImager, 2D resistivity and IP inversion software: Advanced Geosciences, Inc.

Behiry, M.G., and Hanafy, S.M., 2000, Geophysical surveys to map the vertical extension of a sinkhole: a Comparison Study: Symposium on the Application of Geophysics to Engineering and Environmental Problems (SAGEEP-2000, Arlington, VA, Feb. 2000), Powers et al., eds., Environmental and Engineering Geophysical Society, 341-350.

Benson, A.K., Payne, K., and Stubben, M.A., 1997, Mapping groundwater contamination using dc resistivity and VLF geophysical methods–A case study: Geophysics, 62, 80-86.

Bernard, J., and Leite, O., 2004, Multi-electrode resistivity imaging for environmental applications: in Chen, C. and Xia, J. (Eds.), Progress in Environmental and Engineering Geophysics, Proceedings of the 2004 International Conference on Environmental and Engineering Geophysics (ICEEG), June 6–9, Wuhan, China, Science Press USA Inc., 317-322.

Carey, J.S., Frye, J.C., Plummer, N.V., and Swineford, A., 1952, Kansas volcanic ash resources: Kansas Geological Survey, Bulletin, no. 96 (1952 reports of studies), pt. 1, 1-68.

Dawson, C.B., Lane, J.W., Jr., White, E.A., and Belaval, M., 2002, Integrated geophysical characterization of the Winthrop landfill southern flow path, Winthrop, Maine: Symposium on the Application of Geophysics to Engineering and Environmental Problems (SAGEEP) 2002 Annual Meeting of EEGS, Las Vegas, Nevada, February 10-14, 2002, available on CD.

deGroot-Hedlin, C., and Constable, S., 1990, Occam's Inversion to generate smooth, two-dimensional models from magnetotelluric data: Geophysics, 55, 1613-1624.

Edwards, L. S., 1977, A modified pseudosection for resistivity and IP: Geophysics, 42, 1020-1036.

Hardy, R.G., Bauleke, M.P., Hornbaker, A.L., Hess, W.R., and Hladik, W.B, 1965, Kansas industrial mineral development--a feasibility study for the production of filter aids from Kansas volcanic ash: Kansas Geological Survey, Special Distribution Publication, no. 19, 34 p.

Loke, M.H., 2001, Tutorial: 2-D and 3-D electrical imaging surveys. http://www.geoelectrical.com (accessed 13 Mar. 2001).

Oldenburg, D.W., and Li, Y., 1999, Estimating depth of investigation in DC resistivity and IP surveys: Geophysics, 64, 403-416.

Reynolds, J.M., 1997, An introduction to applied environmental geophysics: West Sussex, England, John Wiley & Sons Ltd., 796 p.

Tsourlos, P.I., Szymanski, J.E., and Tsokas, G.N., 1999, The effect of terrain topography on commonly used resistivity arrays: Geophysics, 64, 1357-1363.

Wolfe, J.P, Richard, H., Hauser, E., and Hinks, J., 2000, Identifying potential collapse zones under highways: in Proceedings: Symposium on the Application of Geophysics to Engineering and Environmental Problems (SAGEEP-2000, Arlington, Virginia February 20-24), Environmental and Engineering Geophysical Society, 351-358.

Xia, J., and Miller, R.D., in press, Integrated geophysical survey in defining subsidence features on a golf course: Journal of Geophysics and Engineering.

Zohdy, A.A.R., Eaton, G.P., and Mabey, D.R., 1974, Application of surface geophysics to ground-water investigations: Techniques of Water-Resources Investigations of the United States Geological Survey, book 2, chap. D1, 116 p.